

EFFECT OF NON-LINEAR THERMAL RADIATION, ACTIVATION ENERGY ON HYDROMAGNETIC CONVECTIVE HEAT AND MASS TRANSFER FLOW OF NANOFLUID IN VERTICAL CHANNEL WITH BROWNIAN MOTION AND THERMOPHORESIS IN THE PRESENCE OF IRREGULAR HEAT SOURCES

Dr. Y. Devasena*

Assistant Professor in Mathematics, Department of Basic Sciences and Humanities, School of Engineering and Technology, Sri Padmavathi Mahila Viswavidyalayam, Tirupathi, A.P, India.

Article Received on 12/12/2022

Article Revised on 02/01/2023

Article Accepted on 23/01/2023

***Corresponding Author**

Dr. Y. Devasena

Assistant Professor in Mathematics, Department of Basic Sciences and Humanities, School of Engineering and Technology, Sri Padmavathi Mahila Viswavidyalayam, Tirupathi, A.P, India.

ABSTRACT

An attempt has been made to analyze the impact of thermal radiation, activation energy on convection heat transfer flow of a nanofluid in vertical channel with Brownian motion of thermophoresis in the presence of non-uniform heat sources. By employing Runge-Kutta shooting technique the non linear governing equations have been solved. The velocity, the temperature and nanoparticle concentration have been discussion for different parametric variation. It is found that higher the thermal radiation (Rd) larger the velocity, nano-concentration and smaller temperature. Cf enhances with Rd and

decays with Nr at $\eta=\pm 1$. Nu enhances at left wall and decays at right wall with increase in Rd and Nr. Sh decays at $\eta=-1$ and grows at $\eta=+1$ with Rd and Nr. Velocity, Temperature decay and nanoparticle concentration grows with increase in El. Increase in temperature ratio(A) enhances the velocity, nanoparticle concentration and reduces the temperature

KEYWORDS: Non-linear thermal radiation, Activation energy, Brownian motion, Nanofluid. thermophoresis, Irregular Heat Sources, Vertical channel.

1. INTRODUCTION

Thermal radiation plays a significant role in many engineering applications particularly when the temperature is high. In the case of free convection or when the effect of variable properties are also included, the energy transformation can be a function of difference between T_1 and T_0 . Radiation contributed significantly to the transfer of energy in furnaces, chambers of combustion, rocket plumes, heat exchangers under high temperatures, nuclear reactors and the like. On the other hand, in case of conduction and convection and suppressed, thermal radiation plays an important role during heat transfers even at temperatures of lower degrees like in thermos bottles and space craft thermal control, Makinde^[21], Chiu et al.^[10], Sakurai et al.^[26], Mahapatra et al.^[20], Lee et al.^[18], Liu et al.^[19], Sheikholeslami et al.^[28] have studied free convection flow with thermal radiation and mass transfer through various enclosures.

The model with potential reactants to produce a chemical reaction minimizing the energy in the chemical system is focused nowadays in the industrial manufacturing of, extrusion of plastic, aerodynamics with rubber sheets crystal growing, geothermal or oil reservoir engineering and so on (Dhlamini et al.^[13]). The Arrhenius activation terminology was first indicated by Svante Arrhenius around 1889. One significant measure in free convection boundary layer flows taking into account heat mass transfer together is the specific chemical reactions with finite Arrhenius activation energy. It is more significant to put on the theoretical attempts to predict the advantages of the activation energy inflows mentioned above instead of the experimental works in these areas (Maleque^[22]). But so far, no attempt has been made to explore the dominance of activation energy with velocity slip boundary state on the heat with mass transfer properties of Casson nanofluid flow towards a stretching sheet with magnetic field and non-linear thermal radiation effects. The Netai and Dulal^[23] have been discussed to Influence of Activation Energy and Nonlinear Thermal Radiation with Ohmic Dissipation on hydromagnetic convective heat and mass transfer flow of a Casson Nanofluid over Stretching Sheet.

The study of heat generation or absorption effects in moving fluids is important in view of several physical problems, such as fluids undergoing exothermic or endothermic chemical reactions. The study of natural convection heat transfer induced by internal heat generation has assumed much importance over time due to several applications in geophysics and energy-related engineering problems, such applications include heat removal from nuclear

fuel debris, underground disposals of radioactive waste materials, storage of foodstuff, and exothermic chemical reactions in packed –bed reactor. Acharya and Goldstein^[4], Churbanov et al^[12], Vajravelu and Nayfeh^[31], Chamkha^[9], Grosan et al.^[16], Baker^[6], Sreedevi^[29] extended their studies on assuming different aspects on convective heat transfer induced by internal energy sources, and also have been briefly analysed Sushma V Jakati et al,^[30] & Abou-zeid and Ibrahim^[2] of casson nano MHD flow over a stretching sheet with non-uniform heat source/sink by HAM & Combined effects of variable electrical conductivity and microstructural/multiple slips on MHD flow of micropolar nanofluid over food industries applications.

Heat-transfer enhancement in engineering and industrial systems is one of the hottest topics in research today. With the growing demand for efficient cooling systems, more effective coolants are required to keep the temperature of heat-generating engines and engineering devices such as electronic components below safe limits. In recent time, the use of nanofluids has provided an innovative technique to enhance heat transfer. Nanotechnology has been widely used in engineering and industry, since nanometer-sized materials possess unique physical and chemical properties. The addition of nanoscale particles into the conventional fluids like water, engine oil, ethylene glycol, etc., is known as nanofluid and was firstly introduced by Choi.^[1] Moreover, the effective thermal conductivity of conventional fluids increases remarkably with the addition of metallic nanoparticles with high thermal conductivity. Nanofluids may be considered as single phase flows in low solid concentration because of very small sized solid particles. There are many experimental and theoretical studies on the flow of nanofluids in different geometries (Abo-Eldahab^[1], Abu-Nada^[3], Al-Nimir^[5], Buongiorno^[7], Cebeci et al^[8], Gill et al^[14], Greif^[15]). A numerical study of buoyancy-driven flow and heat transfer of an alumina (Al₂O₃)–water-based nanofluid in a rectangular cavity was done by Hwang et al.^[17] The nanofluid in the enclosure was assumed to be in a single phase. It was found that for any given Grashof number, the average Nusselt number increased with the solid volume concentration parameter. Nield and Kuznetsov^[24] investigated numerically the Cheng–Minkowycz problem for a natural convective boundary-layer flow in a porous medium saturated by a nanofluid. Oztop and Abu-Nada^[25] considered natural convection in partially heated enclosures having different aspect ratios and filled with a nanofluid. They found that the heat transfer was more pronounced at low aspect ratios and high volume fractions of nanoparticles.

Recently, Satya Narayana and Ramakrishna^[27] discussed the effect of Brownian motion and thermophoresis, activation energy on hydromagnetic convective heat transfer flow of nanofluid in a vertical channel.

In the present study, we analyse the combined effects of thermal radiation, activation energy, thermophoresis, Brownian motion, and variable viscosity on the channel flow of water-based nanofluid under the influence of convective heat exchange with the ambient surroundings in the presence of non-uniform heat sources. Such flows are very important in engine cooling, solar water heating, cooling of electronics, cooling of transformer oil, improving diesel generator efficiency, cooling of heat exchanging devices, improving heat-transfer efficiency of chillers, domestic refrigerator and freezers, cooling in machining and in nuclear reactor. In the following sections, the problem is formulated, numerically analysed, and solved. Pertinent results are displayed graphically and discussed.

2. FORMULATION OF THE PROBLEM

Consider the steady flow of an electrically conducting, viscous fluid through a porous medium in a vertical channel by flat walls. A uniform magnetic field of strength H_0 is applied normal to the walls. Assuming the magnetic Reynolds number to be small we neglect the induced magnetic field in comparison to the applied field. The left wall is maintained at constant temperature T_1 and the right wall is maintained at T_2 Newtonian cooling, and concentration C_1, C_0 . We consider a rectangular Cartesian coordinate system $O(x,y)$ with x -axis along the walls and y -axis normal to the walls. The walls are taken at $y = \pm 1$ (Fig.1).

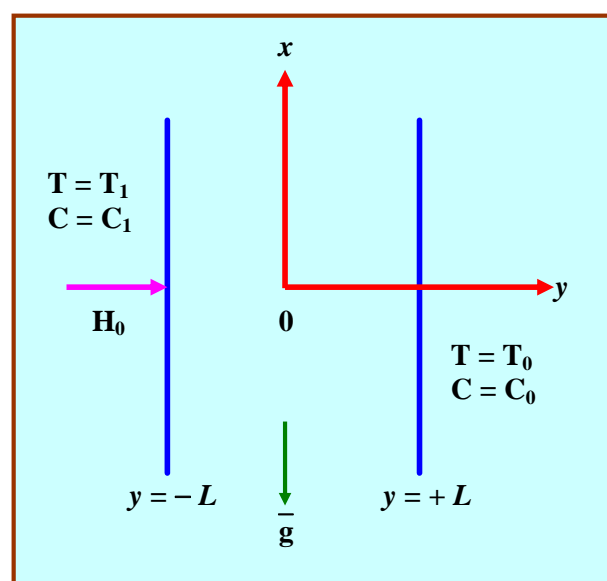


Fig.1. Schematic diagram of the problem under consideration

The boundary layer equations of flow, heat and mass transfer under Boussinesq approximation, and following Buongiorno model^[7] are:

Equation of Continuity

$$\frac{\partial u}{\partial x} = 0 \quad (1)$$

Momentum equation

$$0 = -\frac{\partial p}{\partial x} + \frac{\partial}{\partial y}(\mu_f(T) \frac{\partial u}{\partial y}) - \frac{\sigma B_o^2}{\rho_f} u - \frac{\mu_f(T)}{k_p} u + g[(1 - C_o)\beta\rho_{f_\infty}(T - T_o) - (\rho_p - \rho_{f_\infty})(C - C_o)] \quad (2)$$

Energy equation

$$0 = \alpha_f \frac{\partial^2 T}{\partial y^2} + \left(\frac{\tau}{\rho C_p}\right) \left(D_B \frac{\partial T}{\partial y} \frac{\partial C}{\partial y} + \left(\frac{D_T}{T_m}\right) \left(\frac{\partial T}{\partial y}\right)^2\right) + \left(\frac{1}{\rho C_p}\right) (A_{11}'(T_w - T_o) \frac{\partial f}{\partial y} + B_{11}'(T - T_o)) + \frac{1}{\rho C_p} \frac{\partial(q_r)}{\partial y} \quad (3)$$

Diffusion equation

$$0 = D_B \frac{\partial^2 C}{\partial y^2} + \left(\frac{D_T}{T_m}\right) \frac{\partial^2 T}{\partial y^2} - k_c (C - C_o) \left(\frac{T}{T_o}\right)^n \text{Exp}\left(-\frac{E_n}{kT}\right) \quad (4)$$

The **boundary conditions** relevant to the problem are

$$\begin{aligned} u(-1) = 0, T = T_1, C = C_1 \quad \text{on } y = -L \\ u(+1) = 0, T = T_o, C = C_o \quad \text{on } y = +L \end{aligned} \quad (5)$$

The expression

$$\left(\frac{T}{T_o}\right)^n \text{Exp}\left(-\frac{E_a}{KT}\right) (C - C_o) \quad (6)$$

Is termed as Arrhenius function (1989) with n as a constant exponent, Ea being the activation energy and K, Kr are the Boltzmann constant and chemical reaction term respectively.

The dynamic viscosity of the nanofluids is assumed to be temperature dependent as follows:

$$\mu_f(T) = \mu_o \text{Exp}(-m(T - T_o)) \quad (7)$$

Where μ_o is the nanofluid viscosity at the ambient temperature T_o , m is the viscosity variation parameter which depends on the particular fluid.

Using Roseland approximation the radiative heat flux q_r is given by

$$q_r = \frac{-4\sigma^*}{\beta_R} \frac{\partial}{\partial y} (T^{14}) \quad (8)$$

and expanding T^{14} about T_0 by Taylor's expansion

$$T^{14} = 4T_0^3 T^1 - 3T_0^4$$

The non-dimensional temperature

$$\theta(\eta) = \frac{T - T_0}{T_1 - T_0} \text{ can be simplified as } T = T_0(1 + (\theta_w - 1)\theta) \quad (9)$$

Where $\theta_w = \frac{T_1}{T_0}$ is the temperature ratio. Introducing non-dimensional variables as

$$\eta = \frac{y}{L}, u' = \frac{uL}{\mu_o}, \theta = \frac{T - T_0}{T_1 - T_0}, \phi = \frac{C - C_0}{C_1 - C_0}, p' = \frac{pL^2}{\mu_o^2} \quad (10)$$

On using transformations(7-10) and (2-4), reduces to

The equations (2-4) reduce to

$$\frac{d^2 u}{dy^2} - B \frac{du}{dy} \frac{d\theta}{dy} - Ku + e^{b\theta} (A - M^2 u + Gr(\theta - N\phi)) = 0 \quad (11)$$

$$\left. \begin{aligned} & \frac{d}{d\eta} \left[\left(1 + \frac{4Rd}{3} ([1 + (\theta_w - 1)\theta]^3) \right) \frac{d\theta}{d\eta} \right] + Pr \left(f \frac{d\theta}{d\eta} + Nb \frac{d\theta}{d\eta} \frac{d\phi}{d\eta} + Nt \left(\frac{d\theta}{d\eta} \right)^2 \right) + \\ & + A_{11} f' + B_{11} \theta = 0 \end{aligned} \right\} \quad (12)$$

$$\frac{d^2 \phi}{dy^2} + \left(\frac{Nt}{Nb} \right) \frac{d^2 \theta}{dy^2} - \gamma Sc \phi (1 + n\delta\theta) \text{Exp} \left(-\frac{E_1}{1 + \delta\theta} \right) = 0 \quad (13)$$

The corresponding boundary conditions are

$$\begin{aligned} u(-1) &= 0, \theta(-1) = 1, \phi(-1) = 1 \\ u(+1) &= 0, \theta(+1) = 0, \phi(+1) = 0 \end{aligned} \quad (14)$$

$$\text{where } Gr = \frac{\beta_T g (T_1 - T_0) L^3}{\mu_o^2}, M = \frac{\sigma B_o^2 L^2}{\mu_o}, K = \frac{L^2}{k_p}, N = \frac{\beta_C (C_1 - C_0)}{\beta_T (T_1 - T_0)}, B = m(T_1 - T_0),$$

$$Nb = \frac{\tau D_B (C_1 - C_0)}{\alpha_f}, Nt = \frac{\tau D_T (T_1 - T_0)}{\alpha_f}, A_{11} = \frac{L^2 A'_{11}}{\rho C_p}, B_{11} = \frac{L^2 B'_{11}}{\rho C_p} \theta_w = \frac{T_1}{T_0},$$

$$\delta = \theta_w - 1, E_1 = \frac{E_a}{KT_0}, Rd = \frac{4\sigma^*T_o^3}{3\beta_R k_f}, Sc = \frac{\nu}{D_B}$$

Are the Grashof number, magnetic parameter, Darcy parameter, buoyancy ratio, viscous parameter, Brownian motion parameter, thermophoresis parameter, space dependent heat source parameter, temperature dependent heat source parameter, temperature difference parameter, activation energy parameter, thermal radiation parameter, Schmidt parameter.

3. NUMERICAL ANALYSIS

The coupled non-linear ODEs (11)-(13) along with the corresponding Bc's (14) are solved by employing the RKF algorithm with Mathematica programming. The numerical solutions are carried out by choosing the step size $\Delta\eta=0.001$.

(i) The coupled non-linear system of equations was transformed into a set of first order Des.

$$f = f_1, f' = f_2, f'' = f_3, \theta = f_4, \theta' = f_5, \phi = f_6, \phi' = f_7$$

(ii) The system of first order Des are

$$f''' = (Bf_2f_4 + Kf_1) - e^{Bf_4}(A - M^2f_1 + Gr(f_4 - Nf_6)) \quad (15)$$

$$\theta'' = -\frac{3}{3Rd + 4\{1 + (\theta_w - 1)f_4\}^3} + 4(\theta_w - 1)f_5^2\{1 + (\theta_w - 1)f_4\}^2 + RdPr(Nbf_5f_7 + Ntf_5^2 + A_{11}f_2 + B_{11}f_4) \quad (16)$$

$$\phi'' = -\left(\frac{Nt}{Nb}\right)(f_4f_6 + Nt^2f_4^2 + \gamma Scf_6(1 + n\delta f_4)e^{-E_1(1+\delta f_4)}) \quad (17)$$

The boundary conditions are

$$f_1(\pm 1) = 0, f_4(-1) = 1, f_5(+1) = 0, f_6(-1) = 1, f_6(+1) = 0 \quad (18)$$

(iii) Suitable guess values are chosen for unknown required Bc's.

(iv) RKF technique with shooting method is utilized for step by step integration with the assistance of Mathematica software.

4. SKIN FRICTION, NUSSELT AND SHERWOOD NUMBER:

The quantities of physical interest in this analysis are the skin friction, coefficient C_f , local Nusselt number (Nu), local Sherwood number (Sh) which are defined as

$$C_f = \frac{2\tau_w}{\rho u_w^2}, Nu = \frac{xq_w}{\alpha_f(T_1 - T_o)}, Sh = \frac{xm_w}{D_B(C_1 - C_o)} \quad (19)$$

where

$$\tau_w = \mu \left(\frac{\partial u}{\partial y} \right)_{\eta=\pm 1}, q_w = k_{nf} \left(\frac{\partial T}{\partial y} \right)_{\eta=\pm 1}, m_w = D_B \left(\frac{\partial C}{\partial y} \right)_{\eta=\pm 1} \quad (20)$$

Substituting equation(17) into equation (16),we get

$$Cf = e^{-B\theta} \left(\frac{\partial u}{\partial y} \right)_{\eta=\pm 1}, Nu = - \left(\frac{\partial \theta}{\partial y} \right)_{\eta=\pm 1}, Sh = - \left(\frac{\partial \phi}{\partial y} \right)_{\eta=\pm 1} \quad (21)$$

5. COMPARISON

In the absence of thermal radiation($Rd=0$) the results are good agreement with *Satya Narayana and Ramakrishna*.^[27]

Table 1.

Parameters		Satyanrayana & Ramakrishna ^[27]		Present Results		Satyanrayana & Ramakrishna ^[27]		Present Results	
		$\eta = -1$				$\eta = +1$			
		Nu(-1)	Sh(-1)	Nu(-1)	Sh(-1)	Nu(+1)	Sh(+1)	Nu(+1)	Sh(+1)
B	0.3	0.14162	0.92367	0.14166	0.92369	0.85706	0.11955	0.85709	0.11954
	0.5	0.12762	0.93711	0.12744	0.93717	0.87008	0.10711	0.87009	0.10712
	0.7	0.11472	0.94947	0.11488	0.94949	0.88172	0.09597	0.88173	0.09599
E1	0.1	0.14162	0.92367	0.14168	0.92369	0.85706	0.11955	0.85707	0.11957
	0.3	0.14171	0.91271	0.14174	0.91274	0.85761	0.12292	0.85764	0.12293
	0.5	0.14177	0.90431	0.14178	0.90433	0.85802	0.12551	0.85805	0.12555
Δ	0.2	0.26022	0.82244	0.26034	0.82249	0.71976	0.24821	0.71977	0.24820
	0.4	0.14183	0.94707	0.14188	0.94709	0.85565	0.11422	0.85564	0.11424
	0.6	0.14177	0.95827	0.14179	0.95829	0.86517	0.11655	0.86519	0.11656
Nb	0.2	0.14162	0.92367	0.14166	0.92368	0.85706	0.11955	0.85704	0.11958
	0.3	0.11926	0.83461	0.11929	0.83464	0.90232	0.19255	0.90236	0.19258
	0.4	0.09203	0.77547	0.09209	0.77549	0.96383	0.23907	0.96386	0.23909
Nt	0.1	0.24231	0.93412	0.24233	0.93415	0.74947	0.11949	0.74949	0.11951
	0.3	0.08346	1.41712	0.08347	1.41717	0.98995	0.52933	0.98991	0.52939
	0.5	0.05217	1.76395	0.05218	1.76399	1.07719	1.07865	1.07720	1.07867

6. RESULTS AND DISCUSSION

The aim of this analysis is to study the combined influence of thermal radiation, Activation energy, Brownian motion and thermophoresis on convective heat transfer flow of nanofluid confined in vertical channel in the presence of irregular heat source. The effect of pertinent parameters on flow characteristics have been studied on solving the coupled non-linear governing equations by Runge-Kutta Shooting method.

Figs.2a-2c demonstrate the effect of Grashof number(G) and magnetic parameter(M) on the velocity, temperature and nanoparticle concentration From the profiles we notice that the

velocity, temperature enhance while the nanoparticle concentration reduces in the flow region with increasing values of G . This shows that an increase in G grows the thickness of the momentum, thermal boundary layers and decays solutal layer thickness. With higher the strength of the Lorentz force the velocity decreases and temperature, nanoparticle concentration increase in the flow region. Physically, a retarding force or drag force (Lorentz force) is generated due to the presence of a magnetic force. On the other hand, the heat measure enhances and the mass of the fluid are depicted in figures 2b&2c.

The effect of viscosity parameter(B) and porous parameter(K) on flow variables can be seen from figs.3a-3c. Higher the viscosity parameter(B) larger the velocity, temperature and smaller the nanoparticle concentration in the flow region. An increase in porous parameter(K) depreciates the velocity and temperature, enhances the nanoparticle concentration in the flow region.

Figs.4a-4c demonstrate the effect of thermal radiation (R_d) and Buoyancy ratio(N_r) on flow variables. From the figures we find that higher the radiative heat flux larger the velocity, nanoconcentration and smaller the temperature in the flow region, when the molecular buoyancy force dominates over the thermal buoyancy force the velocity, temperature experience enhancement while nanoparticle concentration depreciates when the buoyancy forces are in the same direction.

The effect of space dependent/temperature dependent heat sources (A_{11}, B_{11}) on flow variables can be seen from figs.5a-5c and 6a-6c. From the profiles we find that the velocity enhances with rising values of space dependent/generating heat source ($A_{11} > 0, B_{11} > 0$). The temperature and nanoconcentration upsurge with space dependent heat source($A_{11} > 0$) and depreciate with heat sink($A_{11} < 0$) (figs.5b&5c). In the presence of heat generating source, energy is generated which results in the enhancement of temperature and nanoconcentration while they decay in the case of absorbing heat source as energy is absorbed in this case(figs.6b&6c)

Figs.7a-7c represent the effect of Brownian motion(N_b) and thermophoresis parameter(N_t) on flow variables. A rise in N_b and N_t leads to a growth in velocity, temperature while nanoparticle concentration grows with N_b and decays with N_t . Physically, thermophoretic force creates a rise in the flow region. Consequently, as N_t increases the thickness of the

momentum, thermal become layers become thicker and solutal layer becomes thinner (figs.7a-7c).

Figs.8a-8c exhibit the effect of temperature excess ratio (A) and activation energy parameter (E_1) on flow variables. Increasing activation energy (E_1) leads to a fall in velocity, temperature and rise in nanoparticle concentration in the flow region. The effect of temperature excess ratio (A) is to enhance velocity, nanoparticle concentration and depreciate temperature and depreciates the temperature in the flow region. This is due to the fact that an increase in temperature relative parameter (A) leads to thickening of the momentum and solutal boundary layers and thinning of the thermal boundary layer.

Lesser the molecular diffusivity/index number (n) larger the velocity, temperature and smaller the nanoparticle concentration (figs.9a-9c). This may be attributed to the fact that increase in Sc and n leads to a growth in momentum and thermal boundary thickness while solutal layer becomes thinner in the flow region.

Figs.10a-10c exhibits the effect of chemical reaction parameter (γ) of on u, θ and ϕ . From the profiles we find that the velocity, temperature increases in both the degenerating /generating chemical reaction cases. The nanoparticle concentration depreciate in both degenerating/generating chemical reaction cases. This may be attributed to the fact that an increase in $\gamma > 0$ leads to growth of momentum, thermal and decays solutal boundary layers.

The skin friction factor (C_f), Nusselt (Nu) and Sherwood number (Sh) at the walls $\eta = \pm 1$ are exhibited in table.2. From the tabular values we observe that the skin friction (C_f) grows at both the walls with increasing values of $G, B, K, Rd, Nt, A, Sc, A_{11} > 0, A_{11} < 0, B_{11} > 0, B_{11} < 0, \gamma > 0$ and $\gamma < 0$ while it decays with rising values of M, Nr, Nb , and E_1 at $\eta = \pm 1$. An increase in heat absorbing source leads to an enhancement in C_f at $\eta = +1$ and reduces at $\eta = -1$. The rate of heat transfer (Nu) enhances with G and reduces with $Sc, n, \gamma > 0$ and $\gamma < 0$ at both the walls. Nu enhances at the left wall ($\eta = -1$) and reduces at the right wall ($\eta = +1$) with higher values of $M, K, Rd, Nr, B_{11} < 0, E_1$ and A . An increase in $B, A_{11} > 0, B_{11} > 0, Nb$ and Nt reduces the rate of heat transfer at the left wall and enhances at the right wall. The rate of mass transfer (Sh) grows at the left wall ($\eta = -1$) and decays at the right wall ($\eta = +1$) with higher values of $G, B, A_{11} > 0, B_{11} > 0, Nt, Sc$ and $\gamma > 0$. Sh reduces at $\eta = -1$ and enhances at $\eta = +1$ with increase in $M, K, Rd, Nr, A_{11} < 0, B_{11} < 0, Nb, E_1, A, n, \gamma < 0$. In addition, $AE(E_1)$ plays an important role in

increasing the local heat transfer coefficient. Generally, AE is the minimum amount of energy that is required for a chemical reaction to stimulates atoms or molecules in the reaction. There should a considerable number of atoms whose AE is less than or equal to translational energy in a chemical reaction, hence in many engineering applications, AE may be considered as a better coolant.

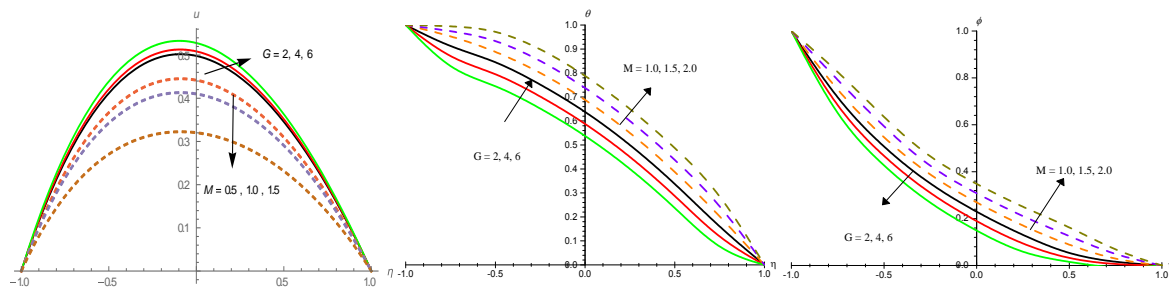


Fig. 2: Variation of [a] velocity(u), [b] Temperature(θ), nano-Concentration(ϕ) with G and M .

$B = 0.25$, $K = 0.2$, $Rd = 0.5$, $Nr = 0.2$, $A_{11} = 0.2$, $B_{11} = 0.2$, $Nb = 0.2$, $Nt = 0.1$, $E_1 = 0.1$, $A = 1.05$, $n = 0.2$, $Sc = 0.24$, $\gamma = 0.5$

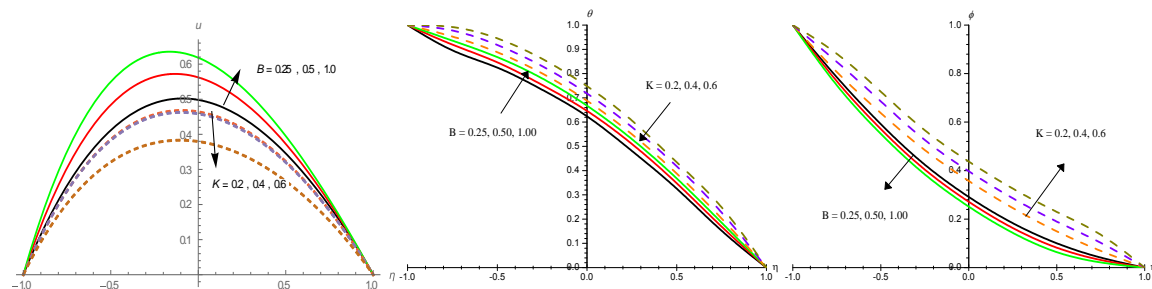


Fig. 3: Variation of [a] velocity(u), [b] Temperature(θ), nano-Concentration(ϕ) with B and K

$G = 2$, $M = 0.5$, $Rd = 0.5$, $Nr = 0.2$, $A_{11} = 0.2$, $B_{11} = 0.2$, $Nb = 0.2$, $Nt = 0.1$, $E_1 = 0.1$, $A = 1.05$, $n = 0.2$, $Sc = 0.24$, $\gamma = 0.5$

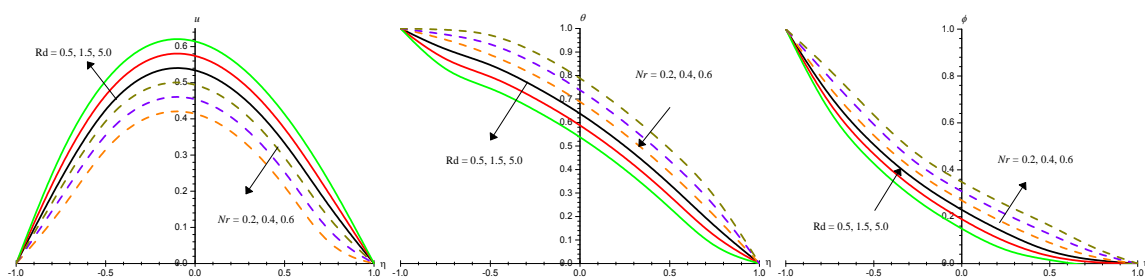


Fig. 4: Variation of [a] velocity(u), [b] Temperature(θ), nano-Concentration(ϕ) with Rd and Nr

$G=2, M=0.5, B =0.25, K=0.2, A_{11}=0.2, B_{11}=0.2, Nb=0.2, Nt=0.1, E_1=0.1, A=1.05, n = 0.2, Sc=0.24, \gamma=0.5$

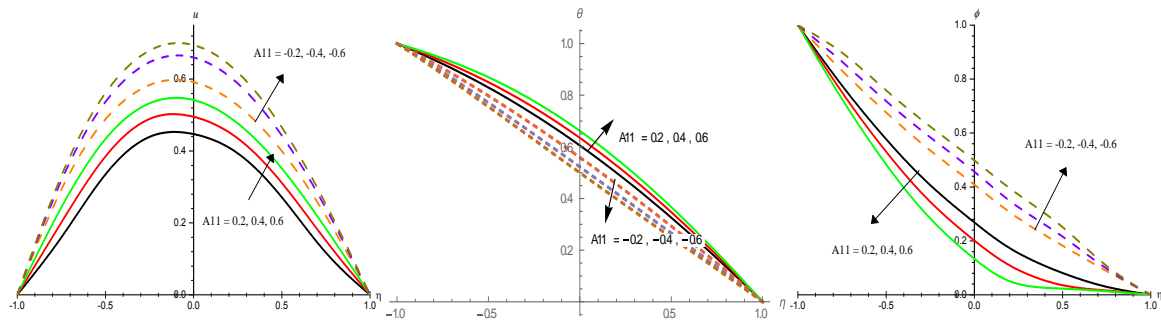


Fig. 5: Variation of [a] velocity(u), [b] Temperature(θ), nano-Concentration(ϕ) with A_{11}
 $G=2, M=0.5, B =0.25, K=0.2, Rd=0.5, Nr=0.2, B_{11}=0.2, Nb=0.2, Nt=0.1,$
 $E_1=0.1, A=1.05, n = 0.2, Sc=0.24, \gamma=0.5$

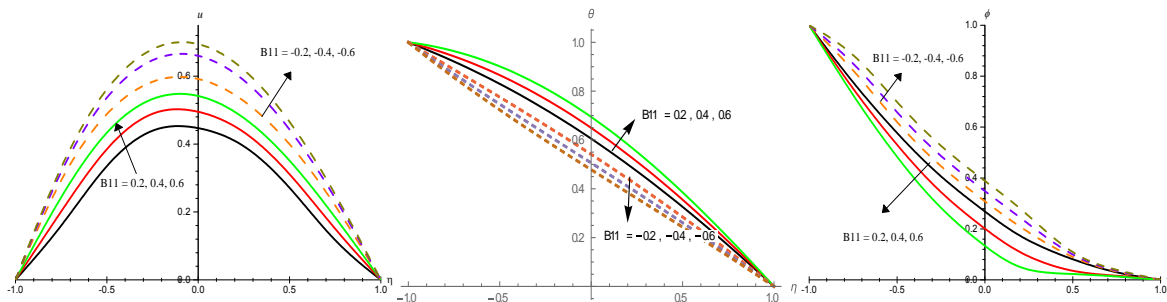


Fig. 6: Variation of [a] velocity(u), [b] Temperature(θ), nano-Concentration(ϕ) with B_{11}
 $G=2, M=0.5, B =0.25, K=0.2, Rd=0.5, Nr=0.2, A_{11}=0.2, Nb=0.2, Nt=0.1,$
 $E_1=0.1, A=1.05, n = 0.2, Sc=0.24, \gamma=0.5$

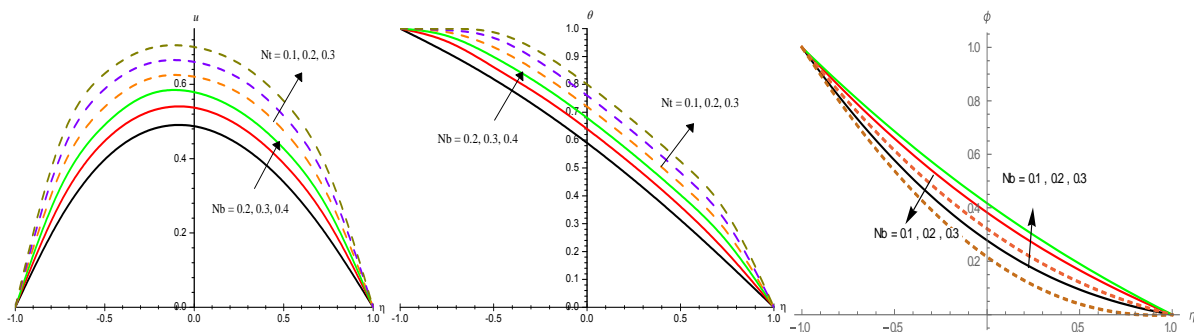


Fig. 7: Variation of [a] velocity(u), [b] Temperature(θ), nano-Concentration(ϕ) with Nb and Nt
 $G=2, M=0.5, B =0.25, K=0.2, Rd=0.5, Nr=0.2, A_{11}=0.2, B_{11}=0.2, E_1=0.1, A=1.05, n =$
 $0.2, Sc=0.24, \gamma=0.5$

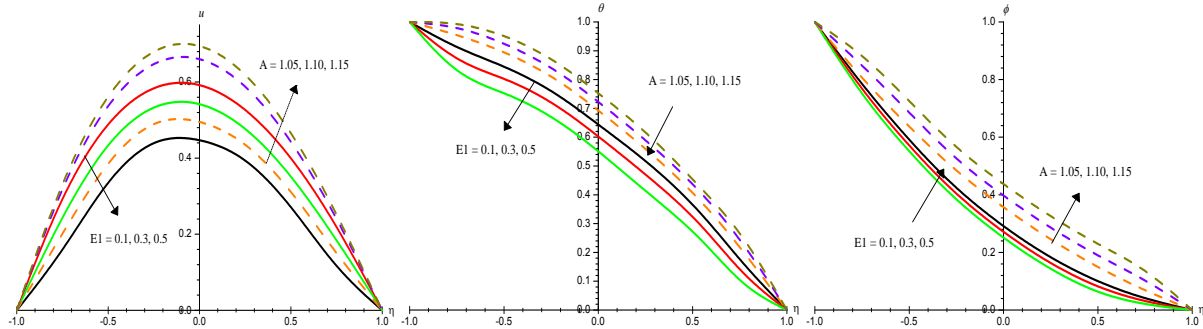


Fig. 8: Variation of [a] velocity(u), [b] Temperature(θ), nano-Concentration(ϕ) with $E1$ and A

$G=2, M=0.5, B =0.25, K=0.2, Rd=0.5, Nr=0.2, A11=0.2, B11=0.2, Nb=0.2, Nt=0.1, n = 0.2, Sc=0.24, \gamma=0.5$

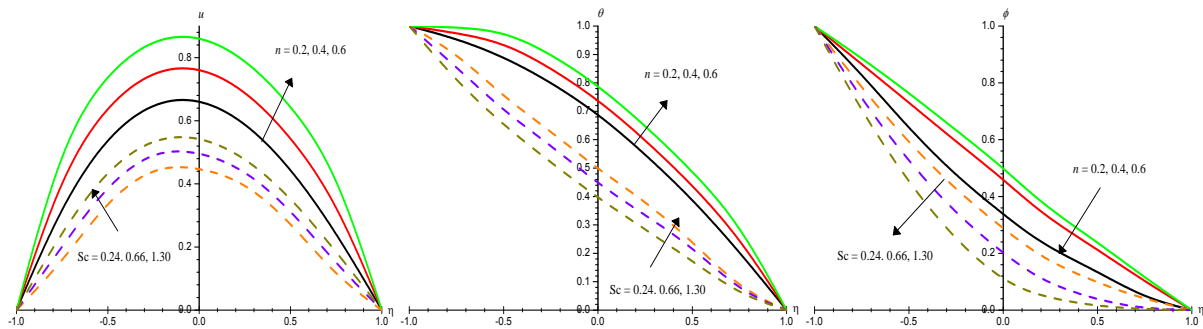


Fig. 9: Variation of [a] velocity(u), [b] Temperature(θ), nano-Concentration(ϕ) with n and Sc

$G=2, M=0.5, B =0.25, K=0.2, Rd=0.5, Nr=0.2, A11=0.2, B11=0.2, Nb=0.2, Nt=0.1, E1=0.1, A=1.05, \gamma=0.5$

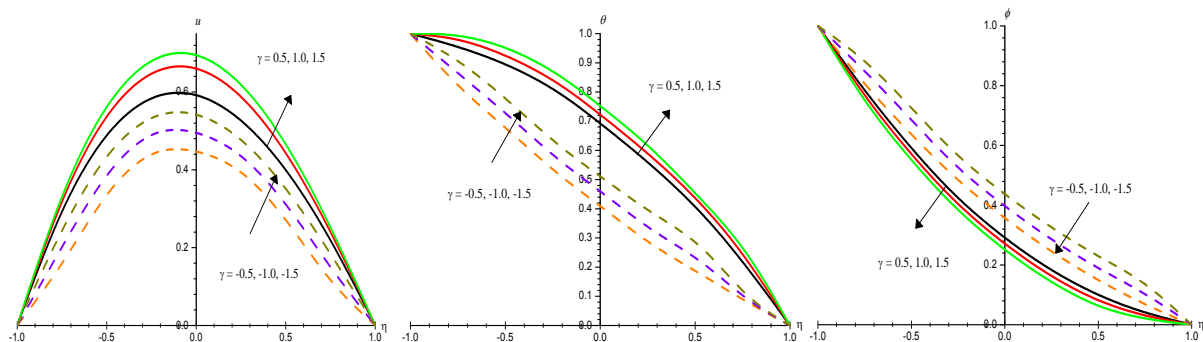


Fig. 10: Variation of [a] velocity(u), [b] Temperature(θ), nano-Concentration(ϕ) with γ

$G=2, M=0.5, B =0.25, K=0.2, Rd=0.5, Nr=0.2, A11=0.2, B11=0.2, Nb=0.2, Nt=0.1, E1=0.1, A=1.05, n = 0.2, Sc=0.24$

Table 2: Skin friction factor(Cf), Nusselt (Nu) and Sherwood number (Sh) at $\eta \pm 1$.

Parameter		Cf(-1)	Cf(+1)	Nu(-1)	Nu(+1)	Sh(-1)	Sh(+1)
G	2	1.23546	-0.869164	0.291988	0.688583	0.744526	0.295501
	4	1.26551	-0.881243	0.291101	0.689454	0.745392	0.294651
	6	1.32124	-0.903692	0.293453	0.691071	0.747001	0.293073
M	0.5	1.12554	-0.794706	0.274353	0.706926	0.761798	0.277525
	1.0	1.08002	-0.765858	0.298767	0.681319	0.737918	0.302593
	1.5	0.89242	-0.636274	0.305872	0.673665	0.730991	0.310073
B	0.25	1.23546	-0.869164	0.291988	0.688583	0.724526	0.295501
	0.5	1.50627	-0.892215	0.285889	0.693541	0.750489	0.290671
	1.0	1.76234	-0.909076	0.280417	0.697847	0.755844	0.286479
K	0.2	1.17155	-0.820184	0.272393	0.708975	0.763709	0.275525
	0.4	1.17994	-0.823572	0.294912	0.685316	0.741678	0.298691
	0.6	1.22008	-0.835061	0.301095	0.678536	0.735654	0.305314
Nr	0.1	1.23546	-0.869164	0.291988	0.688583	0.744526	0.295501
	0.3	1.22559	-0.866547	0.292225	0.688375	0.744295	0.295709
	0.5	1.20587	-0.861308	0.292755	0.687943	0.743831	0.296125
Rd	0.5	1.23209	-0.867458	0.360534	0.620684	0.677424	0.361964
	1.5	1.29018	-0.909101	0.418393	0.568027	0.620736	0.413468
	5	1.30915	-0.915788	0.438092	0.550874	0.601434	0.430239
A11	0.2	1.23546	-0.869164	0.291988	0.688583	0.744526	0.295501
	0.4	1.23779	-0.870335	0.246706	0.737588	0.788684	0.247632
	0.6	1.23994	-0.871414	0.204934	0.782799	0.829416	0.203472
	-0.2	1.23124	-0.867147	0.358826	0.613937	0.679434	0.368377
	-0.4	1.28859	-0.908551	0.420073	0.549988	0.619615	0.430889
	-0.6	1.32654	-0.914758	0.454974	0.512243	0.585576	0.467764
B11	0.2	1.23546	-0.869164	0.291988	0.688583	0.744526	0.295501
	0.4	1.23841	-0.871276	0.192063	0.754335	0.842638	0.231427
	0.6	1.24147	-0.863377	0.093652	0.822308	0.939214	0.165162
	-0.2	1.23087	-0.865755	0.451261	0.598495	0.587953	0.383174
	-0.4	1.28888	-0.906833	0.535332	0.543894	0.505338	0.436434
	-0.6	1.32681	-0.922565	0.606974	0.504222	0.434868	0.475062
Nb	0.1	1.23654	-0.870295	0.314125	0.657934	0.961103	0.123771
	0.2	1.23546	-0.869164	0.291988	0.688583	0.744526	0.295501
	0.3	1.23407	-0.869043	0.263479	0.731487	0.671848	0.351675
Nt	0.2	1.23347	-0.868174	0.293251	0.676485	0.628548	0.405201
	0.3	1.29722	-0.912883	0.273876	0.715588	0.858155	0.177564
	0.4	1.33985	-0.931698	0.252026	0.752648	1.050554	0.039614
E1	0.1	1.23546	-0.869164	0.291988	0.688583	0.744526	0.295501
	0.2	1.23541	-0.869132	0.292064	0.688781	0.737582	0.298292
	0.3	1.23538	-0.869109	0.292121	0.687929	0.732398	0.300381
A	1.05	1.23588	-0.869434	0.269348	0.712379	0.767131	0.272055
	1.10	1.28283	-1.045015	0.283781	0.697442	0.753764	0.286452
	1.15	1.33491	-1.168948	0.291987	0.688519	0.746492	0.294929
Sc	0.24	1.23546	-0.869164	0.291988	0.688583	0.744526	0.295501
	0.66	1.23584	-0.869439	0.291324	0.686845	0.807128	0.271257
	1.30	1.23611	-0.869631	0.290861	0.685628	0.852348	0.254487
<i>n</i>	0.2	1.23588	-0.869433	0.269349	0.712383	0.766988	0.272097

Parameter		Cf(-1)	Cf(+1)	Nu(-1)	Nu(+1)	Sh(-1)	Sh(+1)
	0.4	1.23537	-0.911885	0.289998	0.690723	0.747078	0.293219
	0.6	1.23491	-0.968944	0.291997	0.688545	0.745427	0.295252
γ	0.5	1.23534	-0.869081	0.292188	0.689103	0.726208	0.302824
	1.0	1.23546	-0.869164	0.291988	0.688583	0.744526	0.295501
	1.5	1.23557	-0.869244	0.289103	0.688076	0.762572	0.288387
	-0.5	1.23559	-0.869222	0.688583	0.713943	0.719112	0.290861
	-1.0	1.29502	-0.911632	0.688076	0.692339	0.690735	0.315948
	-1.5	1.33444	-0.968603	0.713943	0.690729	0.669504	0.326147

7. CONCLUSION

The effect of thermal radiation, irregular heat sources, variable viscosity and activation energy on flow characteristics in a vertical channel is analysed. The conclusions of this analysis are

- i) An increase in viscosity parameter(B) enhances the velocity, temperature and reduces nanoparticle concentration. The skin friction, Sherwood number grow, Nusselt number decays with B at the left wall and an opposite effect is observed at the right wall.
- ii) Higher thermal radiation (Rd) larger velocity, nanoconcentration and smaller temperature. Velocity, temperature reduce, nanoconcentration enhances with buoyancy ratio(Nr).Cf enhances with Rd and decays with Nr at $\eta = \pm 1$.Nu enhances at left wall and decays at right wall with increase in Rd and Nr. Sh decays at $\eta = -1$ and grows at $\eta = +1$ with Rd and Nr.
- iii) Velocity, Temperature decay and nanoparticle concentration grow with increase in E1.Increase in temperature ratio(A) grows the velocity, nanoparticle concentration and reduces the temperature. Cf reduces with A and enhances E1. Nu enhances at left wall and reduces at right wall with increase in E1 and A.Sh decays at $\eta = -1$ and grows at $\eta = +1$ with increase in E1 and A.
- iv) Lesser molecular diffusivity/index number(n), larger velocity and temperature, smaller nanoconcentration. Cf, Sh grow, Nu decay with Sc $\eta = \pm 1$.Cf,Sh decay with n at $\eta = -1$ and enhances at $\eta = +1$ while opposite effect is observed in Nu with n at the walls.
- v) Velocity enhances, temperature and nanoparticle concentration reduce in both degenerating/generating chemical reaction cases. Cf enhances, Nu reduces at both walls in both degenerating and generating chemical reaction cases. Sh enhances at $\eta = -1$ and reduces at $\eta = +1$ with $\gamma > 0$.
- vi) The velocity, temperature, nanoparticle concentration enhance with increase in the strength of the space dependent heat source($A_{11} > 0$). Velocity enhances, temperature and

nanoconcentration reduces with $A_{11} < 0$. An increase $B_{11} > 0$, enhances, temperature, nanoconcentration decay while velocity, temperature and nanoconcentration grow with $B_{11} < 0$. C_f grow with $A_{11} > 0$ and $B_{11} > 0$. Nu and Sh decays at left wall and grow at right wall with $A_{11} > 0$ and $B_{11} > 0$.

vii) Brownian motion and thermophoresis exhibit an increasing tendency in velocity, temperature. Nanoconcentration enhances with N_b and reduces with N_t . Rise in N_b decays Nu and Sh while increase in N_t decays Nu and grows Sh at the wall.

8. REFERENCES

1. Abo-Eldahab E. M. Abd El Aziz M. Hall and ion-slip effect on MHD free convective heat generating flow past a semi-infinite vertical flat plate *Phs. Scripta*, 2000; 61: 344.
2. Abou-zeid M.Y., and Ibrahim M.G. (2022): Combined effects of variable electrical conductivity and microstructural/multiple slips on MHD flow of micropolar nanofluid over food industries applications. DOI: <https://doi.org/10.21203/rs.3.rs-1922169/v1>.
3. Abu-Nada E., Application of nanofluids for heat transfer enhancement of separated flows encountered in a backward facing step, *Int. J. Heat Fluid Flow*, 2008; 29: 242–249.
4. Acharya, S and Goldstein, R.J, Natural convection in an externally heated vertical or inclined square box containing internal energy sources, *ASME J. Heat Transfer*, 1985; 107: 855–866.
5. Al-Nimir, M.A., Haddad, O. H: Fully developed free convection in open-ended vertical channels partially filled with porous material, *Journal Porous Media*, 1999; 2: 179-189.
6. Baker, N.A., Karimipour, A and Roslan, R, Effect of Magnetic Field on Mixed Convection Heat Transfer in a Lid-Driven Square Cavity, *J. Thermodynamics*, Article ID 3487182, <http://dx.doi.org/10.1155/2016/3487182>., 2016.
7. Buongiorno J., Convective transport in nanofluids, *J. Heat Transf*, 2006; 128: 240–250.
8. Cebeci, T, Khattab, A. A and LaMont, R: Combined natural and forced convection in a vertical ducts, in: *Proc. 7th Int. Heat Transfer Conf.*, 1982; 3: 419-424.
9. Chamkha, A.J, Non-Darcy fully developed mixed convection in a porous medium channel with heat generation: Absorption and hydromagnetic effects, *Numer. Heat Transfer, Part A*, 1997; 32: 653–675.
10. Chiu, H.C. Jang J.H and Yan W.M. Mixed convection heat transfer in horizontal rectangular ducts with radiation effects, *Int. J. Heat and Mass Transfer*, 2007; 50(15-16): 2874-2882.

11. Choi S.U.S., Zhang Z.G., Yu W., Lockwood F.E., Grulke E.A., Anomalously thermal conductivity enhancement in nanotube suspensions, *Appl. Phys. Lett.*, 2001; 79(2): 2252–2254.
12. Churbanov, A.G., Vabishchevich, P.N., Chudanov, V.V and Strizhov, V.F, A numerical study on natural convection of a heat generating fluid in rectangular enclosures, *Int. J. Heat and Mass Transfer*, 1994; 37: 2969–2984.
13. Dhlamini M., Kameswaran P. K., Sibanda P., Motsa S., and Mondal H., *J. Comp. Design Eng.*, 2019; 6: 149.
14. Gill, W.N. and Del Casal, A: A theoretical investigation of natural convection effects in forced horizontal flows, *AICHE J*, 1962; 8: 513-518.
15. Greif, R., Habib, I.S and Lin, J.C: Laminar convection of a radiating gas in a vertical channel, *J. Fluid. Mech.*, 1971; 46: 513.
16. Grosan, T., Revnic, C., Pop, I and Ingham, D.B, Magnetic field and internal heat generation effects on the free convection in a rectangular cavity filled with a porous medium, *Int. J. Heat Mass Transfer*, 2009; 52: 1525-1533.
17. Hwang K.S., Lee J.-H., Jang S.P., Buoyancy-driven heat transfer of water-based Al₂O₃nanofluids in a rectangular cavity, *Int. J. Heat Mass Transf*, 2007; 50: 4003–4010.
18. Lee J. Jo. D., Chae, H. Chang. S.H., Jeong Y.H. and Jeong J.J. The characteristics of premature and stable critical heat flux for downward flow boiling at low pressure in a narrow rectangular channel, *Experimental Thermal and Fluid Science*, 2015; 69: 86-98.
19. Liu X, Want I and Zhang Z.M. Near field Thermal Radiation Recent progress and outlook, *Naoscale and Microscale Thermophysical Engineering*, 2015; 19(2): 98-126.
20. Mahapatra T.R., Dulal Pal and Mondal S. Unsteady natural convection flow in an inclined enclosure under magnetic field with thermal radiation and heat generation, *Int. Commun. Heat Mass Transfer*, 2013; 41: 47-56.
21. Makinde O.D. Free convection flow with thermal radiation and mass transfer past a moving vertical porous plate, *Int. Commun. Heat Mass Transfer*, 2005; 32(10): 1411-1419.
22. Maleque K.A., *ISRN Thermo.*, 2013; V.9.
23. Netai Roy and Dulal Pal: Influence of Activation Energy and Nonlinear Thermal Radiation with Ohmic Dissipation on hydromagnetic convective heat and mass transfer flow of a Casson Nanofluid over Stretching Sheet, *Journal of Nanofluids*, 2022; 11(6): 819–832, doi:10.1166/jon.2022.1882, www.aspbs.com/jon

24. Nield D.A., Kuznetsov A.V., The Cheng–Minkowycz problem for natural convective boundary-layer flow in a porous medium saturated by a nanofluid, *Int. J. Heat Mass Transf.*, 2009; 52: 5792–5795.
25. Oztop H.F., Abu-Nada E., Numerical study of natural convection in partially heated rectangular enclosures filled with nanofluids, *Int. J. Heat Fluid Flow*, 2008; 29: 1326–1336.
26. Sakurai A Matsubara K, Takakuwa K and Kanbayashi R. Radiation effects on mixed turbulent natural and forced convection in a horizontal channel using direct numerical simulation, *Int. J. Heat and Mass Transfer*, 2012; 55: 2539-2548.
27. Satya Narayana K and Ramakrishna G N Effect of variable viscosity, activation energy and irregular heat sources on convective heat and mass transfer flow of nanofluid in a channel with brownian motion and thermophoresis, *World Journal of Engineering Research and Technology (WJERT)*, 2023; 9: 2. XX-XX, ISSN 2454-695X, SJIF Impact Factor: 5.924, www.wjert.org
28. Sheikholelami M, Hayat T and Alsaedi A: MHD free convection of Al_2O_3 -water nanofluid considering thermal radiation: A numerical study, *Int. J. Heat and Mass transfer*, 2016; 96: 511-524.
29. Sreedevi, Soret and Dufour Effects on Double-Diffusive Heat Transfer Flow in a Rectangular Duct with Radiation Absorption and Non-linear Density-Temperature Relation, *Advances in Applied Research (Pelagia Research Library)*, 2016; 7(4): 127-149.
30. Sushma V Jakati et al, Raju B T, Achala L Nargund, S B Sathyanarayana study of casson nano MHD flow over a stretching sheet with non-uniform heat source/sink by HAM, *International Journal of Mechanical Engineering and Technology (IJMET)*, October, 2018; 9(10): 931-945, Article ID: IJMET_09_10_096, <http://iaeme.com/Home/issue/IJMET?Volume=9&Issue=10> ISSN Print: 0976-6340 and ISSN Online: 0976-6359.
31. Vajravelu, K and Nayfeh, J, Hydromagnetic convection at a cone and a wedge, *Int. Commun. Heat Mass Transfer*, 1992; 19: 701–710.